

## Crossover from Ballistic to Diffusive Thermal Transport in Carbon Nanotubes

Takahiro YAMAMOTO<sup>1\*</sup>, Satoru KONABE<sup>2</sup>, Junichiro SHIOMI<sup>3</sup>, and Shigeo MARUYAMA<sup>3</sup>

<sup>1</sup>*Department of Materials Engineering, The University of Tokyo, 7-3-1 Hongo, Bunkyo-ku, Tokyo 113-8656, Japan* <sup>2</sup>*Department of Physics, Tokyo University of Science, 1-3 Kagurazaka, Shinjuku-ku, Tokyo 162-8601, Japan*

<sup>1</sup>*Department of Mechanical Engineering, The University of Tokyo, 7-3-1 Hongo, Bunkyo-ku, Tokyo 113-8656, Japan*

---

We present a theoretical scheme that seamlessly handles the crossover from fully ballistic to diffusive thermal transport regimes and apply it to carbon nanotubes. At room temperature, the micrometer-length nanotubes belong to the intermediate regime in which ballistic and diffusive phonons coexist, and the thermal conductance exhibits anomalous nonlinear tube-length dependence due to this coexistence. This result is in excellent agreement with molecular-dynamics simulation results showing the nonlinear thermal conductance. Additionally, we clarify the mechanism of crossover in terms of *characteristic frequency*, which is a new concept derived from the scheme.

---

---

\*E-mail address: takahiro@cello.t.u-tokyo.ac.jp

Device heat-generation is a high-priority obstacle to the development of next-generation electronics. Carbon nanotubes (CNTs) are promising candidates, which may alleviate the heating problem because of their high thermal conductivity  $\sim 2000$  W/m-K.<sup>1-5)</sup> This high thermal conductivity originates from a long mean free path of phonons, which is of the order of  $\mu\text{m}$ , even at room temperature.<sup>5,6)</sup> In this situation, where the mean free path is comparable to a typical length of CNTs used in devices, thermal-transport is different than in bulk materials, due to the coexistence of ballistic and diffusive phonons.

One theoretical means of exploring the coexistence phenomena is to use the Keldysh nonequilibrium Green's functions,<sup>7,8)</sup> but it is not well-suited for large-scale calculations. Therefore, we derive a new formula for quasi-ballistic phonon transport, based on a phenomenological approach introduced first by Büttiker for describing inelastic electronic transport in mesoscopic systems.<sup>9)</sup> In the quasi-ballistic regime, phonon-phonon scattering plays an essential role in thermal transport properties, and drives the system toward local thermal equilibrium, with a spatially varying temperature. To describe such an effect phenomenologically, we introduce a fictitious probe connected to a heat reservoir with temperature  $T_F$ , as illustrated in Fig. 1(a).

The fictitious probe extracts a fraction of phonons travelling inside the conductor, and reinjects them into the conductor after thermalization in the reservoir, thus acting effectively as phonon-phonon scattering. In contrast to incoherent phonons propagating from the left to the right lead via the probe, the remaining coherent phonons propagate from the left to right lead without entering the fictitious probe. Thus, the thermal current consists of coherent and incoherent components,  $i_{\text{coh}}(\omega)$  and  $i_{\text{inc}}(\omega)$ , as shown in Fig. 1. Note that the net thermal current flowing in the fictitious probe should be zero:  $\int i_F(\omega)d\omega = 0$ , since the probe is not a real lead, but merely a conceptual one introduced to express phonon-phonon scattering more effectively. In other words, the temperature  $T_F$  at the probe is determined by the condition that no net thermal current flows in the probe.

By performing some basic arithmetic which follows from the fictitious-probe idea, the thermal conductance was found to formally have the same expression as the Landauer formula for coherent phonon transport:<sup>10,11)</sup>

$$\kappa = \sum_{\nu} \int_{\omega_{\nu}^{\text{min}}}^{\omega_{\nu}^{\text{max}}} \frac{d\omega}{2\pi} \hbar\omega \left[ \frac{\partial f(\omega, T)}{\partial T} \right] \mathcal{T}_{\nu}(\omega) \quad (1)$$

even in the presence of phonon-phonon scattering events. Here,  $T$  is an averaged temperature between hot and cold heat baths, and  $\mathcal{T}_{\nu}(\omega)$  is an effective transmission function of a phonon through a conductor, including the phonon-phonon scattering given by

$$\mathcal{T}_{\nu}(\omega) = \zeta_{\nu}^{LR}(\omega) + \frac{\zeta_{\nu}^{FL}(\omega)\zeta_{\nu}^{FR}(\omega)}{\zeta_{\nu}^{LF}(\omega) + \zeta_{\nu}^{FR}(\omega)}, \quad (2)$$

where  $\zeta_{\nu}^{\alpha\beta}(\omega)$  is the transmission function of a coherent phonon with  $\{\nu, \omega\}$  flowing from  $\alpha$

to  $\beta$  leads. Note that we neglect the inelastic component of thermal conductance in Eq. (1), because it gives a negligible contribution to the thermal conductance of CNTs in the quasi-ballistic regime.

Thus far, we have discussed the role of a single probe with temperature  $T_F$ . In general, the temperature inside the conductor varies spatially over a finite range. In order to describe this spatially varying temperature, we introduce a conductor attaching  $N$  probes in series, with respective temperatures  $T_i$  ( $i = 1, 2, \dots, N$ ). For  $N$  probes, the transmission function  $\mathcal{T}_\nu^{\text{tot}}(\omega)$  of a phonon with  $\{\nu, \omega\}$  propagating in a conductor of length  $L$  can be written

$$\mathcal{T}_\nu^{\text{tot}}(\omega) = \frac{\mathcal{L}_\nu(\omega)}{L + \mathcal{L}_\nu(\omega)} \approx \frac{\Lambda_\nu(\omega)}{L + \Lambda_\nu(\omega)}, \quad (3)$$

where  $\mathcal{L}_\nu(\omega) \equiv \mathcal{T}_\nu/\rho(1 - \mathcal{T}_\nu)$  is a characteristic length and  $\rho = N/L$  is the density of scatterers in the conductor. The derivation procedure of Eq. (3) is similar to that of effective transmission for inelastic electronic transport in mesoscopic conductors.<sup>12)</sup> Here, we explain that  $\mathcal{L}_\nu(\omega)$  in Eq. (3) can be regarded as the mean free path  $\Lambda_\nu(\omega) = \tau_\nu(\omega)|v_\nu(\omega)|$ , where  $\tau_\nu(\omega)$  and  $v_\nu(\omega)$  are the backscattering time and group velocity of a phonon with  $\{\nu, \omega\}$ , respectively. The distance between neighboring probes is given by  $dL \equiv L/N = 1/\rho$ . For phonon propagation over the distance  $dL$ , the reflection probability  $\mathcal{R}_\nu(\omega)$  is given by  $\mathcal{R}_\nu(\omega) = (dL/|v_\nu(\omega)|)/\tau_\nu(\omega) = 1/\rho\Lambda_\nu(\omega)$ . Thus, the phonon's mean free path is  $\Lambda_\nu(\omega) = 1/\rho\mathcal{R}_\nu(\omega)$ , and  $\mathcal{L}_\nu(\omega) \approx \Lambda_\nu(\omega)$  in the large- $N$  (or small- $dL$ ) limit where the transmission probability of each small segment with length  $dL$  is close to one ( $\mathcal{T}_\nu(\omega) \approx 1$ ).

As a result, a general expression of thermal conductance is given by

$$\kappa = \sum_\nu \int_{\omega_\nu^{\text{min}}}^{\omega_\nu^{\text{max}}} \frac{d\omega}{2\pi} \hbar\omega \left[ \frac{\partial f(\omega, T)}{\partial T} \right] \frac{\Lambda_\nu(\omega)}{L + \Lambda_\nu(\omega)}. \quad (4)$$

For a short conductor obeying  $L \ll \Lambda_\nu(\omega)$ , Eq. (4) reproduces the Landauer formula<sup>10,11)</sup> for coherent phonon transport with perfect transmission. For a long conductor obeying  $L \gg \Lambda_\nu(\omega)$ , it reduces to the Boltzmann-Peierls formula.<sup>13)</sup>

We now apply the developed formula (4) to thermal transport in CNTs at room temperature. Although the mean free path  $\Lambda_\nu(\omega)$  can be calculated using Eq. (2), we use an phenomenological expression  $\Lambda_\nu(\omega) = c_\nu A/\omega^2 T$  for three-phonon Umklapp scattering events in the low-frequency regime obeying  $\hbar\omega/k_B T \ll 1$ , where  $A = 3.35 \times 10^{23}$  mK/s<sup>2</sup> is the coupling constant for graphene<sup>14)</sup> and  $c_\nu$  is a parameter representing the curvature effect of a CNT ( $c_\nu = 1$  corresponds to a graphene). The use of the phenomenological expression allows us to perform integration in Eq. (4) analytically. Strictly speaking, the phenomenological expression is applicable only to acoustic phonon modes with linear dispersion, but it has been shown to be useful to represent other modes as well.<sup>15)</sup> Consequently the thermal conductance

is expressed simply as:

$$\kappa_{\text{CNT}} = \frac{k_B}{2\pi} \sum_{\nu} \Omega_{\nu} \left\{ \arctan \left( \frac{\omega_{\nu}^{\text{max}}}{\Omega_{\nu}} \right) - \arctan \left( \frac{\omega_{\nu}^{\text{min}}}{\Omega_{\nu}} \right) \right\}, \quad (5)$$

where  $\Omega_{\nu}(L) = \sqrt{c_{\nu}A/TL}$  is a length-dependent characteristic frequency, which is a key quantity for understanding the crossover from ballistic to diffusive phonon transport in the CNTs. The mode- $\nu$  dependence of  $c_{\nu}$  is neglected hereafter, i.e., the mode-dependent characteristic frequency  $\Omega_{\nu}(L)$  is replaced by a mode-independent  $\Omega(L)$ . In spite of the relative simplification, this works remarkably well to describe the length dependence of thermal conductance in the quasi-ballistic regime, as we will discuss below.

In Eq. (3), we did not include effects of phonon scattering at interfaces between a CNT and the left/right leads. One of simple treatments of the interfacial thermal resistance is to introduce it by the following way:  $\kappa^{-1} = \kappa_{\text{CNT}}^{-1} + \kappa_{\text{int}}^{-1}$ . The interfacial resistance  $\kappa_{\text{int}}^{-1}$  can be determined by adjustment to fit experimental data or numerical calculation data.

Now, we estimate the thermal conductance of CNTs by performing nonequilibrium molecular-dynamics (MD) simulations<sup>16,17)</sup> with Brenner's bond-order potential,<sup>18)</sup> and we compare the MD results to the developed theory. The length-dependence of thermal conductance was quantified for various tube lengths, up to micrometers at  $T = 300$  K ( $T_{\text{hot}} = 310$  K and  $T_{\text{cold}} = 290$  K). We refer the detailed simulation procedure to Ref.<sup>17)</sup> The calculated thermal conductances for (3,3) and (5,5) CNTs are shown by blue and red circles in Fig. 2, respectively. The solid curves represent theoretical curves given the proper choice of two parameters  $\kappa_{\text{int}}$  and  $c$  (e.g.,  $\kappa_{\text{int}}^{-1} = 0.09$  K/nW and  $c = 0.65$  for the (3,3) CNT). These curves are in excellent agreement with the MD data. Most recently, the length-dependent thermal conductance (or conductivity) of CNTs shown here has been measured in experiments,<sup>19,20)</sup> although we can not compare the theory with the experiments because the detailed information on tube structure (i.e., number of walls and their chiralities) was not described.

Before turning to detailed discussion of the crossover from ballistic to diffusive transport, it is important to mention that agreement is achieved even without using the long time-scale thermal-current correlations being considered in present theory. In low-dimensional systems, the long time tail of heat-flux autocorrelation has been discussed as contributing to the length dependence and will eventually cause divergence of thermal conductivity.<sup>21,22)</sup> Note that MD simulations potentially include this effect through the coupling of thermal noises, although the onset length for CNTs is not known. Despite this difference between the developed theory and MD simulations, the two are in excellent agreement. Although this agreement cannot be taken as rigorous proof, it empirically suggests that three-phonon scattering events make a major contribution to the length effect in the range of lengths explored by the MD simulations. This is also in agreement with the NEGF calculation results taking higher-order scattering corrections into account.<sup>8)</sup>

Let us return to discussion of the ballistic-diffusive crossover. The thermal-transport properties of CNTs are essentially determined by the relative position of  $\Omega(L)$  with respect to the phonon dispersion relation. As illustrated in Fig. 3, the dashed blue line indicates the position of  $\Omega(L)$  relative to the dispersion relation. As seen in Fig. 2, nanometer-length CNTs display length-independent thermal conductance, reflecting purely ballistic phonon transport. At nanometer length,  $\Omega(L)$  is much larger than the energies of the phonons, as shown in the left panel of Fig. 3.

With increasing  $L$ , up to micrometer length, the value of  $\Omega(L)$  decreases, lying in the middle of the phonon dispersion relation, as shown in the central panel of Fig. 3. In this situation, low-frequency phonon modes with  $\omega_\nu^{\max} \ll \Omega(L)$  give  $L$ -independent thermal conductance reflecting a ballistic nature, whereas the high-frequency modes with  $\omega_\nu^{\min} \gg \Omega(L)$  show  $\kappa \propto 1/L$  reflecting a diffusive nature. The intermediate-frequency phonon modes with  $\omega_\nu^{\min} < \Omega(L) < \omega_\nu^{\max}$  cannot be described in terms of both Landauer and Boltzmann-Peierls formulae, and exhibit nonlinear  $L$ -dependence described by Eq. (5). Thus, we conclude that micrometer-length CNTs belong to the quasi-ballistic thermal transport regime in which ballistic and diffusive phonons coexist.

We next discuss the case when  $\Omega(L)$  is much lower than the excitation frequency of the lowest optical phonons, as shown in the right panel of Fig. 3. In this case, the tube length  $L$  reaches millimeters and the contribution of optical phonons to thermal conductance behaves as  $\kappa \propto 1/L$ , resulting in constant thermal conductivity, as  $\lambda = (L/S)\kappa = \text{const}$ . Here,  $S$  is the cross-sectional area of a CNT. Unlike the optical modes, the acoustic modes, with  $\omega_\nu^{\min} = 0$ , show  $\kappa \propto L^{-1/2}$ , leading to a power-law divergence  $\lambda \propto L^{1/2}$  of thermal conductivity.<sup>15,23)</sup> This power-law behavior is closely related to the long-standing problem pointed out by Pomeranchuk in the 1940s that the low-frequency acoustic phonon contribution to thermal conductivity diverges in the thermodynamic limit  $L \rightarrow \infty$ .<sup>24)</sup> However, it is known, in general, that the divergence disappears if higher-order phonon-phonon scattering events are taken into account, although the possibility of the above-mentioned long-time tail in low-dimensional materials remains an open problem.<sup>21,22)</sup> In either case, the agreement between the current theory and MD simulation results indicates that the higher-order effects are negligible in the current length regime. This agrees with the previously reported observation from Boltzmann's kinetic approach.<sup>15)</sup>

In summary, the current work is the first to derive a theoretical scheme that seamlessly handles the crossover from fully ballistic to diffusive thermal transport regimes. The scheme also bridges the gap between perturbation approaches and MD simulations, which has been an obstacle to establishing a universal theoretical foundation for the study of nanoscale thermal transport. Moreover, the scheme serves as a tool to gain an understanding of the underlying physics, and opens a new path to exploration of novel thermal devices.

T.Y. acknowledges support from the MEXT of Japan through Grants-in-Aid (Nos. 19710083 and 20048008). This work was also supported in part by the Specific Area Research “Carbon Nanotube Nano-Electronics” and by the Global COE Program “Global Center of Excellence for Mechanical Systems Innovation”, MEXT of Japan.

## References

- 1) S. Berber, Y.-K. Kwon, and D. Tomanek, Phys. Rev. Lett. **84**, 4613 (2000).
- 2) P. Kim, L. Shi, A. Majumdar, and P.L. McEuen, Phys. Rev. Lett. **87**, 215502 (2001).
- 3) M. Fujii, X. Zhang, H. Xie, H. Ago, K. Takahashi, T. Ikuta, H. Abe, and T. Shimizu, Phys. Rev. Lett. **95**, 065502 (2005).
- 4) E. Pop, D. Mann, Q. Wang, K. Goodson, and H. Dai, Nano Lett. **6**, 96 (2006).
- 5) C. Yu, L. Shi, Z. Yao, D. Li, and A. Majumdar, Nano Lett. **5**, 1842 (2005).
- 6) J. Hone, M. Whitney, C. Piskoti, and A. Zettl, Phys. Rev. B **59**, R2514 (1999).
- 7) T. Yamamoto and K. Watanabe, Phys. Rev. Lett. **96**, 255503 (2006).
- 8) J.-S. Wang and J. Wang and N. Zeng, Phys. Rev. B **74**, 033408 (2006).
- 9) M. Buttiker, Phys. Rev. B **33**, 3020 (1986).
- 10) L.G.C. Rego and G. Kirczenow, Phys. Rev. Lett. **81**, 232 (1998).
- 11) T. Yamamoto, S. Watanabe, and K. Watanabe, Phys. Rev. Lett. **92**, 075502 (2004).
- 12) S. Datta, *Electronic Transport in Mesoscopic Systems* (Cambridge University Press, Cambridge, England, 1995)
- 13) R.E. Peierls, *Quantum Theory of Solid*. (Oxford University Press, 1955).
- 14) P.G. Klemens and D.F. Pedraza, Carbon **32**, 735 (1994).
- 15) N. Mingo and D.A. Broid, Nano Lett., **5**, 1221 (2005).
- 16) S. Maruyama, Physica B **323** (2002) 193.
- 17) J. Shiomi and S. Maruyama, Jpn. J. Appl. Phys. **47** (2008) 2005.
- 18) D.W. Brenner, Phys. Rev. B **42** (1990) 9458.
- 19) Z.L. Wang, D.W. Tang, X.B. Li, X.H. Zheng, W.G. Zhang, L.X. Zheng, and Y.T. Zhu, Appl. Phys. Lett. **91** (2007) 123119.
- 20) C.W. Chang, D. Okawa, H. Garcia, A. Majumdar, and A. Zettl, Phys. Rev. Lett. **101** (2008) 075903.
- 21) S. Lepri, R. Livi, and A. Politi, Phys. Rep. **377** (2003) 1.
- 22) R. Livi and S. Lepri, Nature **421** (2003) 327.
- 23) J. Wang and J.-S. Wang, Appl. Phys. Lett. **88** (2006) 111909.
- 24) I. Pomeranchuk, J. Phys. (Moscow), **4** (1941) 259.

**Fig. 1.** (color online). The fictitious probes used to describe the phonon-phonon scattering effect. The thermal current through the conductor consists of coherent and incoherent components. The net thermal current through the probe should be zero.

**Fig. 2.** (color online). Length dependence of thermal conductance. The blue and red circles are MD data of the room-temperature thermal conductances of (3,3) and (5,5) CNTs, respectively. The blue and red solid curves represent corresponding theoretical curves (See the text).

**Fig. 3.** (color online). The relative position of the length-dependent characteristic frequency  $\Omega(L) = \sqrt{cA/TL}$  (dashed blue lines) with respect to the phonon dispersions for the (3,3) CNT. Here,  $a$  is the length of a unit cell.



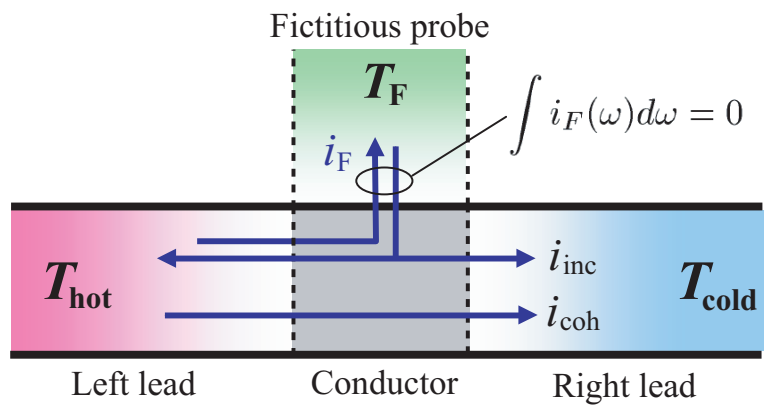


Fig.1

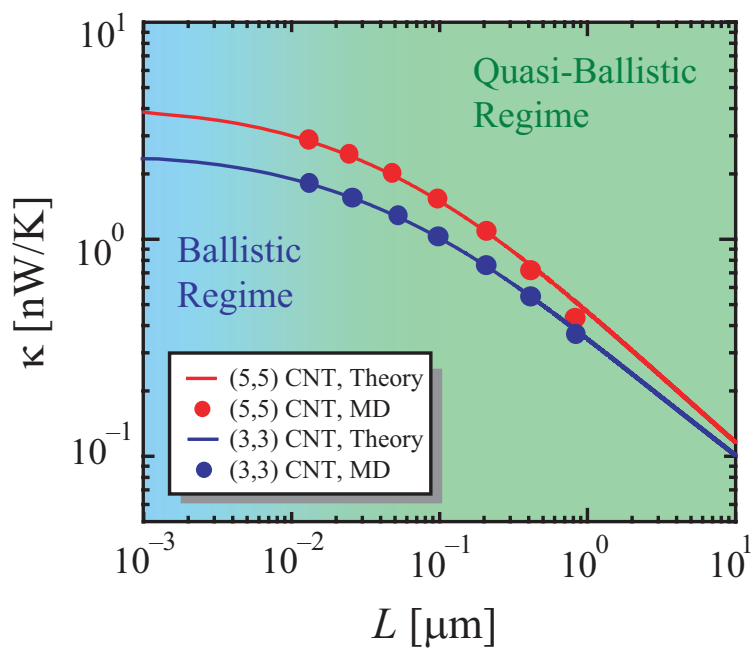


Fig.2

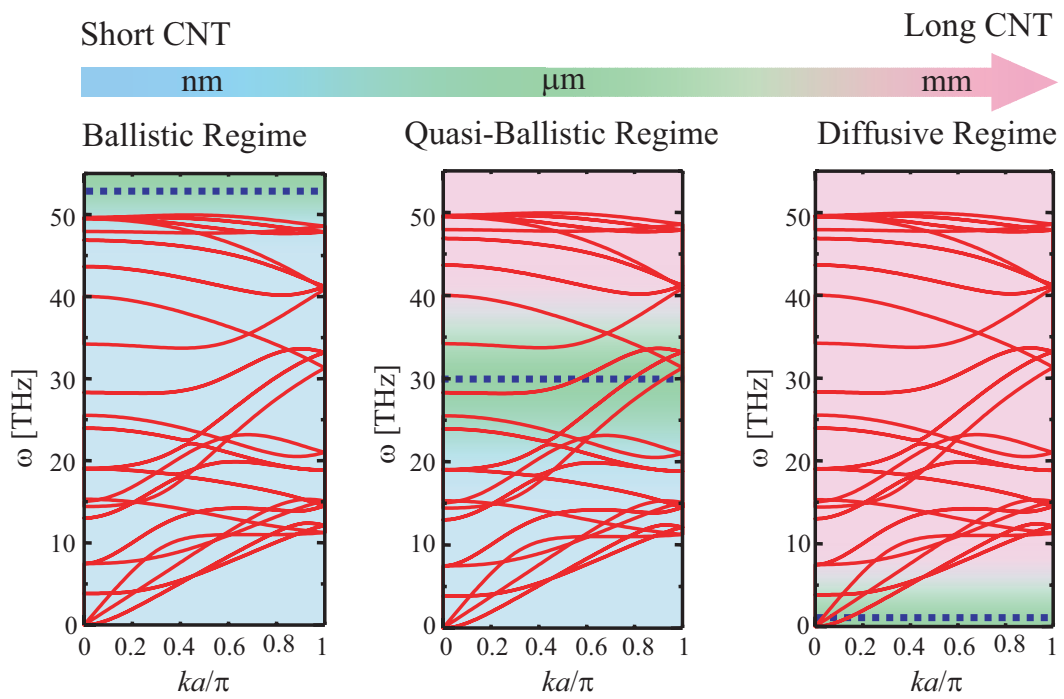


Fig.3